A schematic design of an epidermal touch panel is shown in Fig. 4A. The epidermal touch panel was built on a 1-mm-thick VHB film (3M, Maplewood, MN) so as to insulate the panel from the body. Because VHB film was originally developed as an adhesive, the panel could be attached to an arm without using extra glues (Fig. 4B). The epidermal touch panel was fully transparent so that it could convey visual content behind the touch panel. Moreover, the panel was mechanically soft and stretchable so that a user is comfortable with movement while wearing it. The currents measured before and after attachment are plotted in Fig. 4C. The baseline currents increased after the attachment owing to a leakage of charges through the VHB substrate. The thicker insulating layer generated a smaller baseline current. The effect of thickness of the insulating layers on the baseline currents is shown in fig. S8. The sensitivity to touch decreased after the attachment; however, the touching current was still sufficient to be detected. As shown in Fig. 4D, we subsequently touched from TP#1 to TP#4 on the epidermal touch panel, and the current was measured with the A1 current meter. The correlation between the measured currents and the touched position was not influenced by the attachment. The epidermal touch panel could successfully perceive various motions, such as tapping, holding, dragging, and swiping. Thus, various applications can be easily managed by integrating the panel. As shown in Fig. 4, E to G, writing words (Fig. 4E), playing music (Fig. 4F), and playing chess (Fig. 4G) were accomplished via adequate motions on the epidermal touch panel (movies S3 to S6).

We have demonstrated a highly stretchable and transparent ionic touch panel. We used a PAAm hydrogel containing 2 M LiCl salts as an ionic conductor. We investigated the mechanism of position-sensing in an ionic touch panel with a 1D strip. The ionic touch strip showed precise and fast touch-sensing, even in a highly stretched state. We expanded the position-sensing mechanism to a 2D panel. We could draw a figure using the 2D ionic touch panel. The ionic touch panel could be operated under >1000% areal strain. An epidermal touch panel was developed based on the ionic touch panel. The epidermal touch panel could be applied onto arbitrarily curved human skin, and its use was demonstrated by writing words and playing the piano and games.

REFERENCES AND NOTES

1. T. Young, U.S. patent 5,241,308 (1993).
2. R. Aguilar, G. Meijer, *Proc. IEEE Sens.* **2**, 1360–1363 (2002).
3. S. P. Hotelling, J. A. Strickon, B. Q. Huppi, U.S. patent 7,663,607 (2010).
4. P. T. Krein, R. D. Meadows, *IEEE Trans. Ind. Appl.* **26**, 529–534 (1990).
5. R. Adler, P. J. Desmares, *IEEE Trans. Ultrason. Ferroelectr. Freq. Control* **34**, 195–201 (1987).
6. M. R. Bhalla, A. V. Bhalla, *Int. J. Comput. Appl.* **6**, 12–18 (2010).
7. D. Langley *et al.*, *Nanotechnology* **24**, 452001 (2013).
8. R. Bel Hadj Tahar, T. Ban, Y. Ohya, Y. Takahashi, *J. Appl. Phys.* **83**, 2631–2645 (1998).
9. M. Vosgueritchian, D. J. Lipomi, Z. Bao, . *Adv. Funct. Mater.* **22**, 421–428 (2012).
10. Y. Xia, K. Sun, J. Ouyang, *Adv. Mater.* **24**, 2436–2440 (2012).
11. L. Hu, W. Yuan, P. Brochu, G. Gruner, Q. Pei, *Appl. Phys. Lett.* **94**, 161108 (2009).
12. Z. Wu *et al.*, *Science* **305**, 1273–1276 (2004).
13. J. Zang *et al.*, *Nat. Mater.* **12**, 321–325 (2013).
14. S. Bae *et al.*, *Nat. Nanotechnol.* **5**, 574–578 (2010).
15. L. Hu, H. S. Kim, J.-Y. Lee, P. Peumans, Y. Cui, *ACS Nano* **4**, 2955–2963 (2010).
16. S. De *et al.*, *ACS Nano* **3**, 1767–1774 (2009).
17. C. F. Guo *et al.*, *Proc. Natl. Acad. Sci. U.S.A.* **112**, 12332–12337 (2015).
18. O. Akhavan, E. Ghaderi, *ACS Nano* **4**, 5731–5736 (2010).
19. L. Ding *et al.*, *Nano Lett.* **5**, 2448–2464 (2005).
20. J.-Y. Sun *et al.*, *Nature* **489**, 133–136 (2012).
21. Y. Qiu, K. Park, *Adv. Drug Deliv. Rev.* **64**, 49–60 (2012).
22. M. C. Darnell *et al.*, *Biomaterials* **34**, 8042–8048 (2013).
23. K. Obara *et al.*, *Biomaterials* **24**, 3437–3444 (2003).
24. C. Keplinger *et al.*, *Science* **341**, 984–987 (2013).
25. J. Y. Sun, C. Keplinger, G. M. Whitesides, Z. Suo, *Adv. Mater.* **26**, 7608–7614 (2014).
26. C. Larson *et al.*, *Science* **351**, 1071–1074 (2016).
27. W. Pepper Jr., U.S. patent 4,293,734 (1981).
28. H. Haga *et al.*, *SID Symp. Dig. Tec.* **41**, 669–672 (2010).

ACKNOWLEDGMENTS

This work was supported by the National Research Foundation of Korea (NRF) grant funded by the Korean Government (MSIP) (2015R1A5A1037668). J.-Y.S. and H.-H.L. acknowledge the support of the source technology and materials funded by the Ministry of Trade, Industry and Energy of Korea (MOTIE) (10052783).

SUPPLEMENTARY MATERIALS

www.sciencemag.org/content/353/6300/682/suppl/DC1
Materials and Methods
Figs. S1 to S11
References (*29*–*31*)
Movies S1 to S6

14 April 2016; accepted 19 July 2016
10.1126/science.aaf8810

SLEEP RESEARCH

Local modulation of human brain responses by circadian rhythmicity and sleep debt

Vincenzo Muto,[1,2,3]* Mathieu Jaspar,[1,2,3]* Christelle Meyer,[1,2]* Caroline Kussé,[1,2] Sarah L. Chellappa,[1,2] Christian Degueldre,[1,2] Evelyne Balteau,[1,2] Anahita Shaffii-Le Bourdiec,[1,2] André Luxen,[1,2] Benita Middleton,[4] Simon N. Archer,[5] Christophe Phillips,[1,2,6] Fabienne Collette,[1,2,3] Gilles Vandewalle,[1,2] Derk-Jan Dijk,[5]† Pierre Maquet[1,2,7]†‡

Human performance is modulated by circadian rhythmicity and homeostatic sleep pressure. Whether and how this interaction is represented at the regional brain level has not been established. We quantified changes in brain responses to a sustained-attention task during 13 functional magnetic resonance imaging sessions scheduled across the circadian cycle, during 42 hours of wakefulness and after recovery sleep, in 33 healthy participants. Cortical responses showed significant circadian rhythmicity, the phase of which varied across brain regions. Cortical responses also significantly decreased with accrued sleep debt. Subcortical areas exhibited primarily a circadian modulation that closely followed the melatonin profile. These findings expand our understanding of the mechanisms involved in maintaining cognition during the day and its deterioration during sleep deprivation and circadian misalignment.

Forgoing sleep and staying up at night, be it for professional or recreational reasons, is highly prevalent in modern societies (*1*). Acute sleep loss leads to deterioration of multiple aspects of cognition (*2*) and is associated with increased risk of human errors and health hazards (*3*). These effects are often attributed to the mere lack of sleep. However, despite the progressive buildup of sleep pressure during wakefulness, human performance remains remarkably well preserved until wakefulness is extended into the biological night. This is attributed to a putative circadian alerting signal that increases during the day and reaches its peak in the early evening, close to the rise of melatonin concentration, to counter the mounting homeostatic sleep pressure (*4*–*6*). Cognition deteriorates rapidly and substantially when wakefulness is extended into the night and early morning hours. This is attributed to the accumulated sleep pressure and the dissipation of the circadian alerting signal (*6*, *7*). Whether and how this interaction between homeostatic sleep pressure and circadian rhythmicity is represented at the regional brain level is not known. Single–time

[1]GIGA-Cyclotron Research Centre–In Vivo Imaging, University of Liège, Liège, Belgium. [2]Walloon Excellence in Life Sciences and Biotechnology (WELBIO), Liège, Belgium. [3]Psychology and Cognitive Neuroscience Research Unit, University of Liège, Liège, Belgium. [4]Faculty of Health and Medical Sciences, University of Surrey, Guildford, UK. [5]Sleep Research Centre, Faculty of Health and Medical Sciences, University of Surrey, Guildford, UK. [6]Department of Electrical Engineering and Computer Science, University of Liège, Liège, Belgium. [7]Department of Neurology, CHU Liège, Liège, Belgium.
*These authors contributed equally to this work. †These authors contributed equally to this work. ‡**Corresponding author. Email: pmaquet@ulg.ac.be**

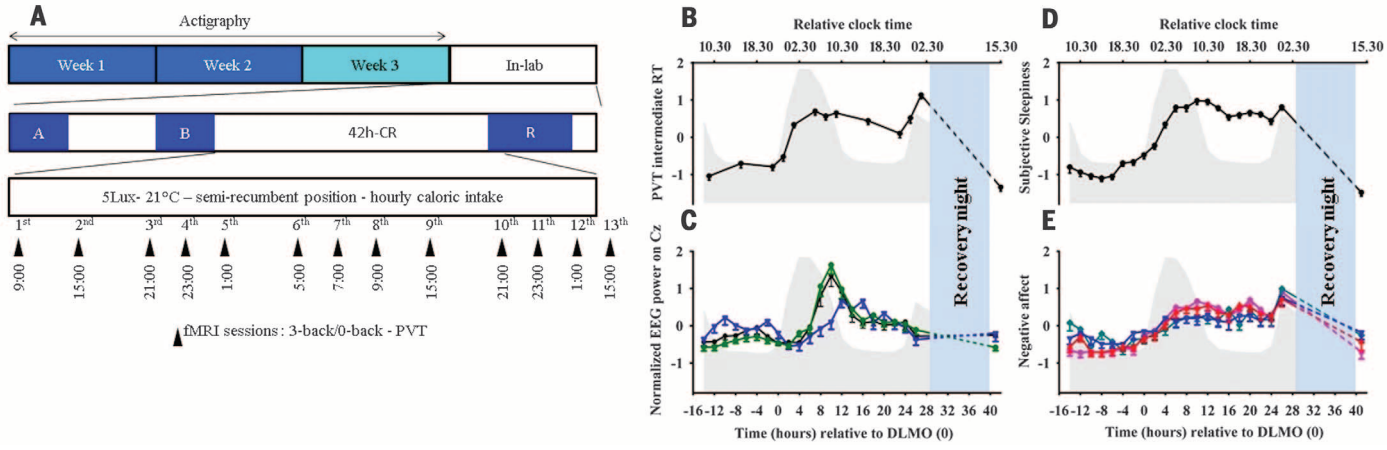

Fig. 1. Experimental protocol, behavioral, and physiological results. (**A**) Schematic representation of the experimental protocol. Actigraphy was recorded during 3 weeks prior to the laboratory study, which comprised an 8-hour adaptation night (A), an 8-hour baseline night (B), and a 12-hour recovery night (R). After baseline night, participants maintained wakefulness for 42 hours under constant conditions in dim light and in a semi-recumbent position (*12*). Note the clustering of the fMRI sessions in the morning (sessions 6 to 8) and evening (sessions 3 to 5 and 10 to 12). (**B** to **E**) Physiological and behavioral data, realigned to DLMO. The gray area illustrates the mean melatonin profile; the blue area represents the recovery sleep episode. All data are normalized z-scores, mean values ± SEM. (B) PVT Intermediate reaction times varied significantly across the 13 fMRI sessions ($F_{12, 366}$ = 55.52, P < 0.0001). (C) Waking EEG power in delta (0.75 to 4.5 Hz, black line), theta (4.75 to 7.75 Hz, green line), and alpha (8 to 12 Hz, blue line) frequency bands. A main effect of time relative to DLMO was detected for delta ($F_{21, 577}$ = 8.44, P < 0.0001), theta ($F_{21, 576}$ = 18.86, P < 0.0001), and alpha power ($F_{21, 572}$ = 3.32, P < 0.0001). (D) Subjective sleepiness varied significantly with time relative to DLMO ($F_{21, 629}$ = 58.51, P < 0.0001). (E) Subjective status: stress (cyan; main effect of time relative to DLMO: $F_{21, 628}$ = 5.06, P < 0.0001), anxiety (blue; $F_{21, 629}$ = 3.34, P < 0.0001), happiness (red; $F_{21, 629}$ = 9.86, P < 0.0001), and motivation (pink; $F_{21, 630}$ = 13.59, P < 0.0001). Higher scores indicate higher levels of stress, anxiety, unhappiness, and demotivation.

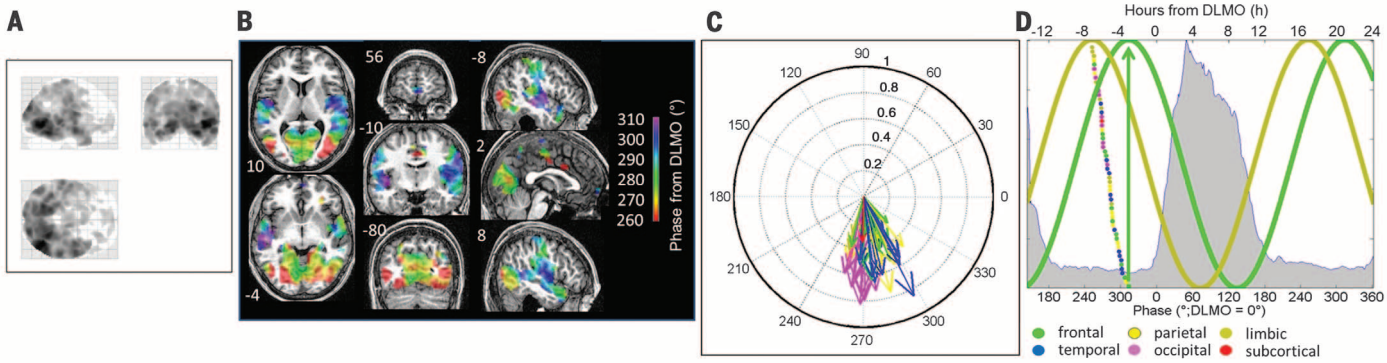

Fig. 2. PVT fMRI analysis 1. (**A**) Transparent brain display in Montreal Neurological Institute (MNI) space of areas showing significant responses with 24-hour periodicity estimated with the Sandwich Estimator method (*21*) (P < 0.05, FDR over the whole brain). (**B**) Circadian phase map of brain responses to PVT (P < 0.05, FDR over the whole brain). The local response phase is displayed according to the color scale (°, DLMO = 0°) and overlaid over an individual normalized T1 MR scan. Coordinates are in millimeters along *z*, *y*, and *x* axes. (**C**) Polar representation of response phases (°, DLMO = 0°). Arrow colors correspond to the color key in (D). (**D**) Predicted time courses of 24-hour period responses expressed as phase and approximate hours from DLMO. Mean melatonin profile is shown in gray. Sine waves illustrate the earliest (beige, amygdala) and latest (green, inferior frontal gyrus) response timing. Between these two extreme phases, the staggered dots correspond to the timing of significant regional peak responses. These responses were grouped in six different areas according to the color code. Limbic phases ranged from 252° to 284°; occipital, 255° to 270°; frontal, 255° to 313°; parietal, 255° to 308°; temporal, 266° to 302°. Subcortical area consisted of left thalamus (coordinates, –18 –30 –2; phase, 268°).

point assessments of human brain responses to various cognitive tasks after acute sleep loss have demonstrated changes consistent with sleep loss' detrimental influence on brain information processing (*8*). However, an assessment of the time course of brain responses during sleep loss is currently not available.

We used repeated functional magnetic resonance imaging (fMRI) sessions to assess whether brain responses are modulated by circadian rhythmicity during sustained wakefulness, and how circadian rhythmicity interacts with the sleep pressure accumulated with elapsed time awake and its dissipation during recovery sleep. Young healthy volunteers (17 men, 16 women; age 21.12 ± 1.7) stayed awake under constant environmental and behavioral conditions for a 42-hour period. The experiment started in the morning and covered two biological days, a full biological night, and the beginning of a second biological night. Brain responses were assessed in 12 fMRI sessions clustered in the morning (hours ~05 to 09) and the evening/early night (hours 21 to 01), two periods characterized by rapid changes in the circadian modulation of cognitive performance. A 13th fMRI session took place after recovery sleep (Fig. 1A).

Circadian phase was determined from the central circadian pacemaker–driven melatonin rhythm (*9*), which showed a typical profile with low levels during the day and a sudden increase in the late

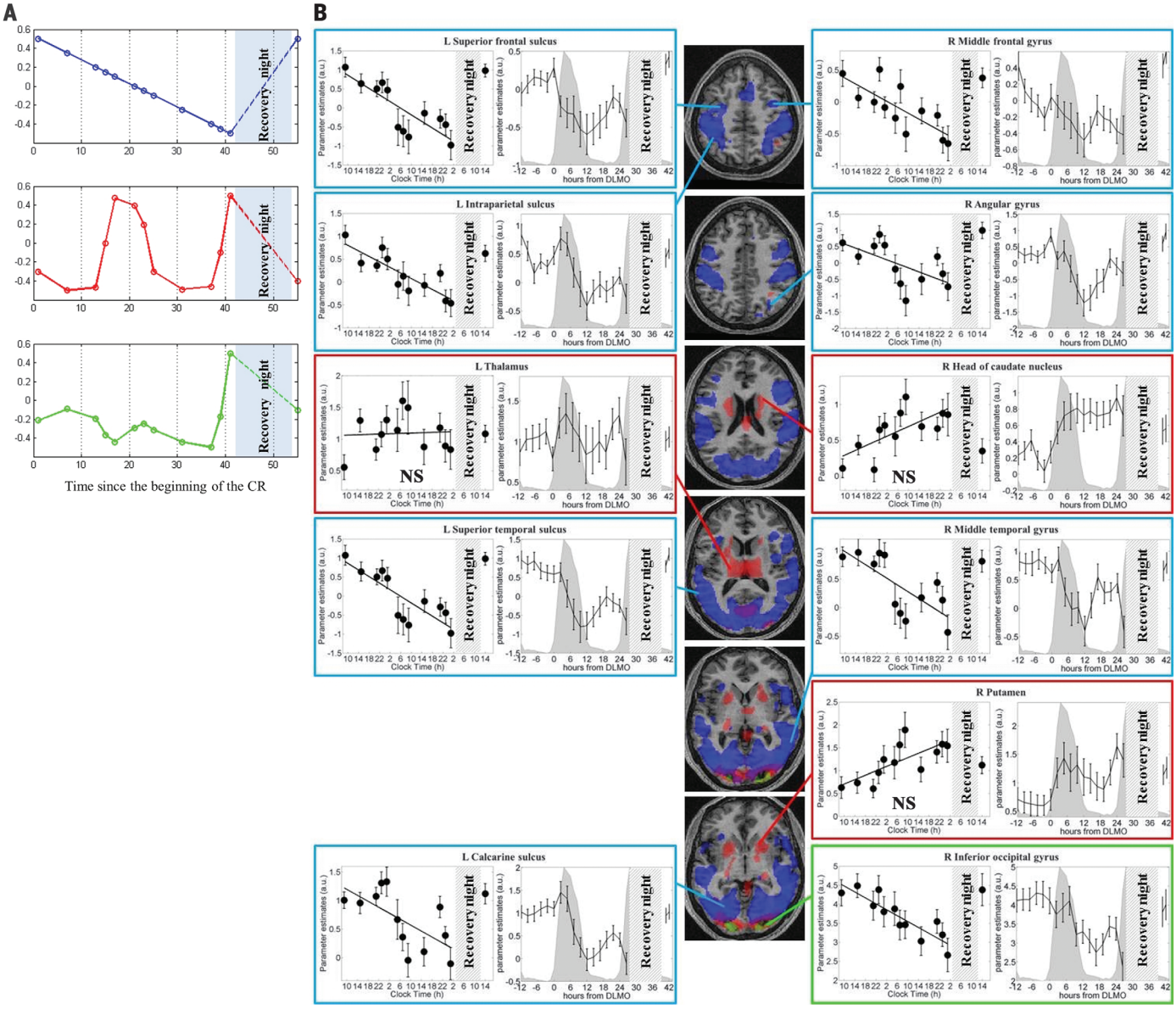

Fig. 3. PVT fMRI analysis 2. (**A**) Illustration of dimensionless fixed-effects fMRI contrasts testing (from top to bottom) a decrease in response with increasing sleep pressure during wakefulness and its recovery after sleep (blue), their fluctuation in association with mean melatonin level (red), and the interaction between these two factors (green). Note that the interaction is characterized by a steady level of response up to the evening sessions of day 3. (**B**) Images show significant effects of homeostatic sleep pressure (blue), circadian rhythmicity (red), and their interaction (green), displayed at $P < 0.05$ (FWE) over an individual normalized T1-weighted MR scan. Left and right panels provide two different representations of the time course of brain responses, which were significant for sleep debt (blue border), circadian (red border), or the interaction (green border) contrasts. Irrespective of the contrast, beta estimates are plotted against clock time (left panels; linear regression is computed with respect to time awake during the sleep deprivation period) and time relative to DLMO (right panels; mean melatonin levels are shown in gray; activity estimates have been interpolated every 2 hours 24 min from hour –12 to hour +28). Coordinates are expressed in millimeters along *z* axis. NS, not significant.

evening hours [mean dim-light melatonin onset (DLMO), 22:33 ± 00:09 (SEM)]. Sleep during the 12-hour recovery night following the sleep deprivation was characterized by shorter sleep latency, increased sleep efficiency, total sleep time, and rapid eye movement (REM) and non-REM sleep, thereby confirming the increase in sleep pressure relative to baseline (tables S1 and S2).

Subjective sleepiness, negative affect, and delta and theta electroencephalographic (EEG) power increased with elapsed time awake and returned to baseline after recovery sleep. These variables also showed a circadian modulation, with poorest ratings observed at the end of the biological night (at approximately 8:00 a.m.) and at the end of the sleep deprivation (at approximately 01:00 a.m.)—that is, after melatonin had risen again (Fig. 1, C to E).

During fMRI sessions, participants performed the psychomotor vigilance task (PVT) (*10*), which generated data on reaction times to pseudo-randomly occurring low-frequency stimuli (*11*). Reflecting the effects of elapsed time awake and circadian phase, performance remained relatively stable during the first day, significantly declined after the first and second melatonin onsets, partially recovered during the second day, and returned to baseline after recovery sleep (Fig. 1B) (*12*).

A first fMRI voxelwise analysis identified any significant circadian periodicity in brain response profiles by combining two orthogonal regressors: 24-hour period sine and cosine waves adjusted to individual DLMO and computed for each individual

scan time. A significant circadian modulation was detected in a large set of cortical areas, involving nearly the whole cortical mantle [$P < 0.05$, false discovery rate (FDR) over the whole brain; Fig. 2A and table S3], with the exception of the dorsolateral prefrontal cortex.

Analyses of response phase showed significant variation across brain regions (Friedmann test, $\chi^2 = 30.13$, df = 4, $P = 4.60 \times 10^{-6}$) and a range spanning ~250° to ~320° relative to melatonin secretion onset (DLMO), with maximum responses occurring earlier in occipital and allocortical areas (amygdala and cingulate cortex) than in multimodal association areas (precuneus, temporal cortex, and prefrontal areas; Fig. 2, B to D). The predicted response profiles peaked during the subjective afternoon and reached their nadir in the second part of the night, up to the early morning hours, close to the offset of melatonin levels (Fig. 2D).

Although this analysis established a circadian modulation of regional brain responses, it assumed that the latter fluctuated as a sine wave—an assumption that does not correspond to actual time courses of most circadian biomarkers (*12*, *13*). A second analysis evaluated the circadian modulation of PVT brain responses using an empirical marker of the circadian process: the mean melatonin level across volunteers (Fig. 3A, red). We simultaneously assessed whether brain responses to the PVT were modulated by accumulating sleep pressure (blue) and how circadian rhythm and homeostatic sleep pressure interact (green). Because no pure marker of homeostatic sleep pressure can be derived from empirical data obtained during sleep deprivation, its effect was modeled as monotonically decreasing with elapsed time awake and increasing after recovery sleep (*12*), as empirically observed (*14*) and usually modeled (*15*).

This second analysis indicated that the time course of responses significantly correlated with mean melatonin levels in a number of subcortical areas (midbrain, cerebellum, basal ganglia, and thalamus) and in a few cortical areas (primary sensorimotor cortices, occipital pole, and intraparietal sulcus), confirming a significant main effect of circadian rhythm in these regions (Fig. 3B, red areas, and table S5). In these areas, there was no significant effect of sleep debt. A significant negative effect of sleep debt was observed in a large set of cortical areas that spanned high-order association cortices of the frontal, parietal, insular, and cingulate cortices as well as visual and sensorimotor cortices (Fig. 3B, blue areas, and table S4). Their response pattern showed a decrease in response to elapsed time awake, with a return to baseline levels after recovery sleep (Fig. 3B, blue areas, and table S4). Their parameter estimates, adjusted to melatonin onset, also revealed a substantial (although not significant) circadian modulation, characterized by a rapid decrease in responses during the late subjective night or early subjective morning, around the melatonin offset. The circadian modulation appears more tightly in phase with melatonin levels in posterior areas than in more anterior areas, accounting for the significant interaction between sleep pressure and circadian rhythmicity observed in occipital poles and thalamic areas (Fig. 3B, green areas, and table S6). Note that a transient increase of modeled cortical responses was no longer located in the "circadian" afternoon (as seen in analysis 1) but instead appeared immediately before the onset of melatonin secretion (Fig. 3B, response time courses relative to DLMO in frontal, parietal, and temporal cortices), a circadian time associated with low sleep propensity known as the wake maintenance zone (*6*).

Brain responses to an *n*-back task were also recorded during fMRI sessions. Executive responses (3-back > 0-back) in the bilateral anterior insula were significantly modulated by a circadian oscillation, synchronous to the melatonin rhythm [$P < 0.05$, familywise error (FWE) over the whole brain] (*12*) (fig. S1). This finding rules out a global task-independent circadian influence and suggests the influence of a local, region-specific, task-dependent circadian signal.

These findings reveal a pervasive effect of circadian rhythmicity and homeostatic sleep pressure on cortical responses during a sustained attention task. The interaction between circadian signals and sleep debt was formally proven in occipital areas, although inspection of response time courses suggests that both factors influence responses of many more cortical areas (Fig. 3B, right panels).

It appears that the respective influence of sleep debt and circadian rhythmicity is more balanced in posterior cortical areas, whereas sleep debt exerts a disproportionately larger influence in more anterior, associative areas. However, this generalization should be confirmed by further experimental data based on various cognitive tasks that are differentially affected by sleep loss and circadian rhythmicity (*2*).

More important, our results demonstrate a regional modulation of brain circadian rhythmicity. Several subcortical responses show a strong circadian modulation but no significant influence of sleep debt. By contrast, in most cortical areas, sleep pressure exerts a widespread negative influence on regional responses. This differential regulation of brain responses might explain the supposedly "compensatory" responses repeatedly reported in thalamic areas during sleep loss (*8*). In the morning after sleep deprivation (8 to 12 hours after DLMO, the typical assessment time point in fMRI studies of acute sleep deprivation), thalamic and striatal responses are indeed larger than in cortical areas. However, these strong thalamic responses might not reflect a compensation for the detrimental effects of accumulating sleep debt; they may merely indicate a dependency of cortical and subcortical response amplitude on the circadian phase (Fig. 3B). This observation highlights the importance of considering circadian phase when investigating the effects of sleep loss on brain mechanisms.

There is also a local modulation of cerebral circadian phase. This suggests that the circadian rhythmicity imposed by the master clock, located in the suprachiasmatic nucleus of the hypothalamus, can to some extent be locally altered, potentially in response to task-related requirements. The mechanisms of this local modulation are unknown. Local changes in clock gene expression (*16*, *17*) or posttranslational circadian mechanisms may be involved. Clock gene expression is sensitive to neuronal metabolic changes [e.g., redox state (*18*, *19*)] and is altered in response to sleep debt (*20*).

These data demonstrate that sleep homeostasis and circadian rhythmicity affect brain responses, in accordance with current views on the regulation of sleep and waking performance. They also require a reformulation of these views to include the relative contributions of circadian rhythmicity and homeostatic sleep pressure to regionally specific (i.e., local) brain function. Our findings have implications for the understanding of the brain mechanisms underlying the maintenance of daytime cognitive performance and its deterioration, as observed in shift work, jet lag, sleep disorders, aging, and neurodegenerative diseases.

REFERENCES AND NOTES

1. E. Bixler, *Sleep Med.* **10** (suppl. 1), S3–S6 (2009).
2. J. C. Lo *et al.*, *PLOS ONE* **7**, e45987 (2012).
3. S. M. Rajaratnam, J. Arendt, *Lancet* **358**, 999–1005 (2001).
4. D. J. Dijk, T. L. Shanahan, J. F. Duffy, J. M. Ronda, C. A. Czeisler, *J. Physiol.* **505**, 851–858 (1997).
5. J. K. Wyatt, A. Ritz-De Cecco, C. A. Czeisler, D. J. Dijk, *Am. J. Physiol.* **277**, R1152–R1163 (1999).
6. D. J. Dijk, C. A. Czeisler, *Neurosci. Lett.* **166**, 63–68 (1994).
7. D. J. Dijk, J. F. Duffy, C. A. Czeisler, *J. Sleep Res.* **1**, 112–117 (1992).
8. M. W. Chee, L. Y. Chuah, *Curr. Opin. Neurol.* **21**, 417–423 (2008).
9. P. Pevet, E. Challet, *J. Physiol. Paris* **105**, 170–182 (2011).
10. D. F. Dinges, J. W. Powell, *Behav. Res. Methods Instrum. Comput.* **17**, 652–655 (1985).
11. M. Basner, D. F. Dinges, *Sleep* **34**, 581–591 (2011).
12. See supplementary materials on *Science* Online.
13. C. Czeisler, O. M. Buxton, in *Principles and Practice of Sleep Medicine*, M. Kryger, T. Roth, W. Dement, Eds. (Elsevier, 2011), pp. 402–411.
14. J. K. Wyatt, C. Cajochen, A. Ritz-De Cecco, C. A. Czeisler, D.-J. J. Dijk, *Sleep* **27**, 374–381 (2004).
15. P. Achermann, *Aviat. Space Environ. Med.* **75** (suppl.), A37–A43 (2004).
16. X. Yu *et al.*, *Curr. Biol.* **24**, 2838–2844 (2014).
17. L. E. Chun, E. R. Woodruff, S. Morton, L. R. Hinds, R. L. Spencer, *J. Biol. Rhythms* **30**, 417–436 (2015).
18. T. A. Wang *et al.*, *Science* **337**, 839–842 (2012).
19. G. Asher *et al.*, *Cell* **134**, 317–328 (2008).
20. P. Franken, D. J. Dijk, *Eur. J. Neurosci.* **29**, 1820–1829 (2009).
21. B. Guillaume, X. Hua, P. M. Thompson, L. Waldorp, T. E. Nichols, *Neuroimage* **94**, 287–302 (2014).

ACKNOWLEDGMENTS

Supported by Fonds National de la Recherche Scientifique (Belgium), Actions de Recherche Concertée of the Wallonia-Brussels Federation, University of Liège research funds, Fondation Médicale Reine Elisabeth, Fondation Simone et Pierre Clerdent, Bial Foundation, FEDER-Radiomed, and a Royal Society Wolfson Research Merit Award (D.-J.D.). We thank B. Guillaume for help in setting up the SWE analysis, E. Lambot and A. Golabek for assistance in data collection, and C. Schmidt for valuable feedback on the manuscript. Data are archived on CRC servers and available upon request. The authors report no conflict of interest.

SUPPLEMENTARY MATERIALS

www.sciencemag.org/content/353/6300/687/suppl/DC1
Materials and Methods
Supplementary Text
Tables S1 to S6
Figs. S1 and S2
References (*22*–*51*)

25 September 2015; accepted 20 June 2016
10.1126/science.aad2993

Local modulation of human brain responses by circadian rhythmicity and sleep debt

Vincenzo Muto, Mathieu Jaspar, Christelle Meyer, Caroline Kussé, Sarah L. Chellappa, Christian Degueldre, Evelyne Balteau, Anahita Shaffii-Le Bourdiec, André Luxen, Benita Middleton, Simon N. Archer, Christophe Phillips, Fabienne Collette, Gilles Vandewalle, Derk-Jan Dijk and Pierre Maquet (August 11, 2016)

Science **353** (6300), 687-690. [doi: 10.1126/science.aad2993]

Editor's Summary

Circadian rhythms and sleep deprivation

Sleep deprivation, such as that experienced because of shift work, jet lag, sleep disorders, and aging, leads to deterioration of many aspects of health. Cognition deteriorates rapidly and substantially when we stay awake through the night. To investigate the time course of brain responses during sleep loss, Muto *et al.* scanned volunteers repeatedly during an extended period of wakefulness (see the Perspective by Czeisler) in which circadian and homeostatic drives differentially affected local brain regions.

Science, this issue p. 687; see also p. 648

Science (print ISSN 0036-8075; online ISSN 1095-9203) is published weekly, except the last week in December, by the American Association for the Advancement of Science, 1200 New York Avenue NW, Washington, DC 20005.